Cell Death and Differentiation (2013) 20, 1089–1100

www.nature.com/cdd

A human iPSC model of Ligase IV deficiency reveals an important role for NHEJ-mediated-DSB repair in the survival and genomic stability of induced pluripotent stem cells and emerging haematopoietic progenitors

K Tilgner[1,2], I Neganova[1,2], I Moreno-Gimeno[3], JY AL-Aama[4], D Burks[3], S Yung[1,2], C Singhapol[5], G Saretzki[5], J Evans[1], V Gorbunova[6], A Gennery[7], S Przyborski[8], M Stojkovic[9], L Armstrong[1,2], P Jeggo[10] and M Lako*[,1,2]

DNA double strand breaks (DSBs) are the most common form of DNA damage and are repaired by non-homologous-end-joining (NHEJ) or homologous recombination (HR). Several protein components function in NHEJ, and of these, DNA Ligase IV is essential for performing the final 'end-joining' step. Mutations in *DNA Ligase IV* result in LIG4 syndrome, which is characterised by growth defects, microcephaly, reduced number of blood cells, increased predisposition to leukaemia and variable degrees of immunodeficiency. In this manuscript, we report the creation of a human induced pluripotent stem cell (iPSC) model of LIG4 deficiency, which accurately replicates the DSB repair phenotype of LIG4 patients. Our findings demonstrate that impairment of NHEJ-mediated-DSB repair in human iPSC results in accumulation of DSBs and enhanced apoptosis, thus providing new insights into likely mechanisms used by pluripotent stem cells to maintain their genomic integrity. Defects in NHEJ-mediated-DSB repair also led to a significant decrease in reprogramming efficiency of human cells and accumulation of chromosomal abnormalities, suggesting a key role for NHEJ in somatic cell reprogramming and providing insights for future cell based therapies for applications of LIG4-iPSCs. Although haematopoietic specification of LIG4-iPSC is not affected *per se*, the emerging haematopoietic progenitors show a high accumulation of DSBs and enhanced apoptosis, resulting in reduced numbers of mature haematopoietic cells. Together our findings provide new insights into the role of NHEJ-mediated-DSB repair in the survival and differentiation of progenitor cells, which likely underlies the developmental abnormalities observed in many DNA damage disorders. In addition, our findings are important for understanding how genomic instability arises in pluripotent stem cells and for defining appropriate culture conditions that restrict DNA damage and result in *ex vivo* expansion of stem cells with intact genomes.
Cell Death and Differentiation (2013) **20**, 1089–1100; doi:10.1038/cdd.2013.44; published online 31 May 2013

DNA damage occurs frequently and the absence of DNA repair can lead to cell death, genomic instability and cancer.[1] The most serious form of damage, DNA double strand breaks (DSBs) arises predominantly through ionizing radiation (IR), cytotoxic drugs, replication errors and endogenous reactive oxygen species. Non-homologous-end-joining (NHEJ) and homologous recombination (HR) are used to repair DSBs.[2,3] In mammalian cells, NHEJ is the major DSB repair pathway,[2] by which two ends are re-joined after limited end processing. Several protein components function in NHEJ[4] (KU70/KU80, DNA-PKcs, DNA Ligase IV, XRCC4, XLF and Artemis) and of these, DNA Ligase IV is an essential component that performs the final 'end processing' step of NHEJ.[5,6] In the absence of classical NHEJ factors or low availability of DNA-PKcs, an alternative end joining pathway known as microhomology-mediated-end joining (MMEJ) operates.[7] This pathway utilises poly (ADP-ribose) polymerase I (PARP-1), histone H1 and Ligase III/XRCC1 (but not DNA-PKcs) for repairing the DSBs and is characterised by slower repair kinetics and lower repair fidelity when compared with the classical NHEJ.

Defects in DSB repair can lead to cancer predisposition, immune dysfunction, radiosensitivity, developmental delay and neurodegeneration.[8,9] In particular, inherited defects in NHEJ-mediated-DSB repair, account for ~15% of human severe combined immunodeficiencies.[4] *Lig4* and *Xrcc4* null mutations are embryonic lethal, hence it is likely that human mutations are hypomorphic.[10–14] Mutations is one of the key components of the NHEJ complex, *DNA Ligase IV* result in a

[1]Institute of Genetic Medicine, International Centre for Life, Newcastle University, Newcastle, UK; [2]NESCI, Newcastle University, Newcastle, UK; [3]Centro de Investigacion Principe Felipe, Valencia, Spain; [4]Princess Al Jawhara Al-Brahim Center of Excellence in Research of Hereditary Disorders, King Abdulaziz University, Jeddah, Saudi Arabia; [5]Institute for Ageing and Health, Newcastle University, Newcastle, UK; [6]Department of Biology, University of Rochester, Rochester, NY, USA; [7]Institute of Cellular Medicine, Newcastle University, Newcastle, UK; [8]School of Biological and Biomedical Sciences, Durham University, Durham, UK; [9]Human Genetics Department, Medical Faculty, University of Kragujevac, Kragujevac, Serbia and [10]Genome Damage and Stability Centre, University of Sussex, Brighton, UK
*Corresponding author: M Lako, Institute of Genetic Medicine, International Centre for Life, Newcastle University, Central Parkway, Newcastle NE1 3BZ, UK. Tel: +44 191 241 8688; Fax: +44 191 241 8666; E-mail: Majlinda.Lako@ncl.ac.uk
Keywords: non homologous end joining (NHEJ); double strand break (DSB); induced pluripotent stem cells (iPSC); human pluripotent stem cells; Ligase IV deficiency; ionising radiation (IR)
Abbreviation: NHEJ, Non homologous end joining; DSB, double strand break; iPSC, induced pluripotent stem cells; HR, homologous recombination; IR, ionising radiation; MMEJ, microhomology-mediated-end joining; ESC, embryonic stem cells
Received 26.10.12; revised 17.3.13; accepted 09.4.13; Edited by B Zhivotovsky; published online 31.5.13

clinical condition, named LIG4 Syndrome (OMIM 606593), which is characterized by growth defects, microcephaly, reduced number of blood cells, increased predisposition to leukaemia and variable degrees of immunodeficiency.[15–17] There is substantial phenotypic variation between LIG4 patients, likely due to the nature of the mutation, which determines the level of ligase activity and ability to repair NHEJ-mediated-DSBs.[18]

The ability to repair DSBs is especially important for adult stem cells, which are responsible for tissue replenishment in long-lived multi-cellular organisms. This is best exemplified in the haematopoietic system, which is maintained by small numbers of haematopoietic stem cells (HSCs) in the bone marrow and which by requirement of their function must maintain their genomic stability at all costs. As such, defects in various forms of DNA repair pathways must have deleterious consequences for these cells. This has been proven experimentally: for example, mice deficient in one of the NHEJ core machinery components, Ku80, DNA-PKcs or polymerase μ show reduced numbers of haematopoietic progenitors in the bone marrow, as well as an age-related decrease of HSC reconstitution.[19,20,21] Hypomorphic Lig4 mice display a profound immunodeficiency, an age-dependent decrease in HSC numbers, impaired self-renewal function of long-term adult HSCs, reduced bone marrow cellularity and lower numbers of erythrocyte precursors, as well as a severe block in B and T cell development.[13,22,23] Together these data suggest that HSCs accumulate DSBs during ageing, but most importantly rely on the NHEJ-mediated-DSB repair pathway in maintaining homoeostasis. Indeed, a recent report has shown that NHEJ is the main DSB repair pathway in quiescent HSCs.[24]

A similar stringent requirement for the maintenance of genomic stability must hold true for embryonic stem cells (ESCs) as they give rise to all cell types present in adult organism. Previous work done by our group has shown that both human and mouse ESC possess efficient DNA repair and reactive oxygen species scavenging ability; however, this stress defence capability is downregulated during their differentiation.[25,26] Both HR and NHEJ (but not MMEJ) have been suggested to function in human ESC and the more recently generated human induced pluripotent stem cells (iPSCs) to maintain this genomic stability;[27,28] however, the impacts of dysfunctional NHEJ or HR have not been assessed either at the pluripotent stage or during their differentiation. In this manuscript, we have taken advantage of iPSC technology and have created a human iPSC model of LIG4 deficiency to investigate the impacts of deficient NHEJ on pluripotent stem cell renewal and their differentiation to haematopoietic lineages. An in depth study of this model reveals that NHEJ-mediated-DSB repair is important for the survival and maintenance of genomic stability of both human iPSC and emerging haematopoietic progenitors derived therefrom.

Results

Derivation and characterisation of LIG4-iPSC. We created an *in vitro* model of LIG4 deficiency using iPSC technology. Fibroblasts from three LIG4 patients carrying different mutations in the *DNA LIGASE IV* gene and unaffected controls were transduced with lentiviruses expressing a polycistronic OSKM (*OCT4, SOX2, KLF4, c-MYC*; Table 1) cassette. Of the three fibroblasts strains, F07/614 and GM17523 have the lowest NHEJ-mediated-DSB repair activity as described in.[18] The third LIG4 fibroblast sample, GM16088 has 5–10% of DSB ligase activity,[18,29] thus conferring a milder DSB repair phenotype, when compared to F07/614 and GM17523. p53 deficiency has been shown by others to rescue the embryonic lethality, neuronal apoptosis and fibroblast proliferation/senescence

Table 1 Summary of iPSC lines derived from LIG4 patients together with mutation status and reprogramming efficiency

Patient ID	Nature of mutation/ligase activity	Number of established lines/method	Reprogramming efficiency	Name of iPSC line
F07/614	Homozygous: **A3V/T9I/R278H:** this mutation yields DNA LIGASE IV protein with no detectable adenylation or ligation activity	1 iPSC line/polycystronic OSKM	0.002%	**F07/614 iPSC LIG4**
F07/614	Homozygous/**A3V/T9I/R278H:** this mutation yields DNA LIGASE IV protein with no detectable adenylation or ligation activity	6 iPSC lines/ polycystronic OSKM + **p53 shRNA-mediated knockdown**	0.06%	**F07/614 iPSC LIG4-p53$^-$**
GM17523	Compound heterozygote: **G469E:R814X G469E** mutation yields DNA LIGASE IV protein with no detectable ligation activity; **R814X** mutation results in DNA LIGASE IV truncated protein, which is barely detectable most likely due to non-sense mediated decay	1 iPSC line/polycystronic OSKM	0.012%	**GM17523 iPSC-LIG4**
GM16088	Homozygous **R278H:** this mutation reduces DNA LIGASE IV adenylation and ligase activity to about 5–10% of wild-type protein	6 iPSC lines/polycystronic OSKM	0.05%	**GM16088-iPSC LIG4**
Neonatal human dermal fibroblasts (NHDF)	**Normal**	16 iPSC lines/polycystronic OSKM	0.3%	**NHDF-iPSC control**

Bold highlight the mutation of each patient.

defects of Lig4 mouse mutants.[11] In addition, p53 knockdown has been shown to enhance the somatic cell reprogramming process.[30] To investigate further the effects of p53 depletion in the context of human *LIG4* mutations, we generated LIG4/p53-deficient patient-specific fibroblasts by shRNA-mediated lentiviral transduction of F07/614 LIG4 fibroblasts (Supplementary Figure 1A) and subjected them to iPSC-mediated reprogramming (Table 1).

Our results showed that LIG4 fibroblasts generated iPSC with lower efficiency when compared with controls suggesting a role for NHEJ-mediated-DSB repair during cellular reprogramming of somatic cells to pluripotency (Table 1). Knockdown of p53 in LIG4 fibroblasts increased this reprogramming efficiency, but not to the same extent as the unaffected controls (Table 1). To investigate whether phenotypic reversion could occur by exogenous expression of *DNA LIGASE IV*, we generated one stable iPSC line (GM17523 + LIG4) by nucleofection of a plasmid construct containing the full length cDNA of *DNA LIGASE IV* gene followed by antibiotic selection into the GM17523-iPSC (Supplementary Figure 1B). All resulting iPSC were morphologically indistinguishable from human ESC and expressed all the tested pluripotent markers (Figure 1a). Transient expression of Cre-recombinase resulted in successful excision of transgene (Figures 1b and c). All LIG4-iPSC carried the *DNA LIGASE IV* mutations (Figure 1d) and were genetically identical to the respective patient fibroblasts (Supplementary Figure 2). We performed karyotype analysis on parent fibroblasts and resulting iPSC and observed three interesting phenomena: first, iPSC with a normal karyotype were derived from parent fibroblasts, which consisted of a mixture of cells with normal and abnormal karyotypes (refer to F07/614 iPSC and fibroblasts), presumably due to selective pressure (Figure 1e); second, LIG4-iPSCs lines were prone to accumulation of chromosomal abnormalities even when derived from fibroblasts with a normal karyotype (refer to GM17523 fibroblasts and resulting iPSCs clone in Figure 1e), suggesting a role for NHEJ-mediated-DSB repair in the maintenance of genomic stability during somatic cell reprogramming; third, *DNA LIGASE IV* overexpressing iPSC lines with normal karyotype could be generated from LIG4 patient-specific iPSC consisting of a mixture of cells with normal and abnormal karyotypes, presumably due to selective pressure (refer to GM17523-iPSC and GM17523-iPSC + LIG4 in Figure 1e).

To confirm the pluripotency of LIG4- and control-iPSC, *in vitro* differentiation studies were performed as described in the Materials and Methods section, followed by immunocytochemical analysis with markers specific for each germ layer (Figure 2A). Specific staining was observed for all three markers in all LIG4- and control-iPSC lines; however, there were differences in the expression pattern of intermediate filament DESMIN and the microtubule constituent β-III-Tubulin (TUJ1) in LIG4-iPSC-derived cells (for example control NHDF-iPSC line showed a characteristic β-III-Tubulin staining along neurite-like outgrowths generated from the differentiation of this line, while those were missing in all LIG4-iPSC-derived cells; Figure 2A), suggesting an altered cytoskeletal structure in the patient-specific LIG4-iPSC lines. These differences in expression pattern of the cytoskeletal markers were reversed in the p53-deficient LIG4-iPSC line (F07/614/p53- iPSC) and *DNA LIGASE IV* overexpressing LIG4 patient-specific iPSC (GM17523-iPSC + LIG4). *In vivo* tests of pluripotency, which involve subcutaneous injections of iPSC into immuno-compromised mice revealed that none of the LIG4-iPSC lines were able to give rise to teratomae. In contrary, the human ESC (H9 line), unaffected control-iPSC line and *DNA LIGASE IV* overexpressing LIG4 patient-specific iPSC (GM17523-iPSC + LIG4) formed typical teratomae comprised cells derived from all three germ layers (Figure 2B). Together these data suggest that there are essential *in vitro* and *in vivo* phenotypic differences between LIG4-and control-iPSC lines, which are due specifically to *DNA LIGASE IV* mutations, rather than likely artefacts associated with the reprogramming process and iPSC differentiation.

Impacts of deficient NHEJ-mediated DSB repair on human iPSC. To assess the impact of different *DNA LIGASE IV* mutations on NHEJ-mediated DSB repair ability of human iPSC, we carried out measurement of NHEJ and HR activity using fluorescent constructs that allow sensitive measurements of DSB repair efficiency.[31] This analysis demonstrated a significant reduction in NHEJ-DSB repair activity in all LIG4-iPSC lines, which could be reversed by overexpression of *DNA LIGASE IV* (Figure 3a). All three LIG4 patient-specific fibroblasts included in this study have been reported to have different levels of remaining ligase activity due to the nature of their specific mutations (Table 1). Our results showed that this differential NHEJ activity is also preserved in the LIG4-iPSC with GM17523 and F07/614 showing the lowest NHEJ-mediated DSB repair (Figure 3a). The reduction in NHEJ activity was accompanied by increased HR in the LIG4-iPSC lines (Figure 3a) suggesting some cross-talk between the DSB repair pathways as already reported.[32,33]

Literature precedence suggests that both HR and NHEJ are utilized in human ESC and iPSC to repair DSBs; however, the main pathway used to repair DSBs caused by IR is high-fidelity NHEJ.[27,28] To investigate the impacts of deficient NHEJ-mediated-DSB repair, we subjected all iPSC lines to IR and analysed the impacts by immunofluorescent microscopy analysis of DSB site specific phosphorylated H2A.X (γH2A.X) at different time points (Figures 3b–d). This analysis shows that all LIG4-iPSC lines are deficient in their DSB repair activity and are unable to repair the IR-caused damage even after 24 hours, despite the higher HR capacity (Figure 3a). In contrast, human ESC and control iPSC can initiate repair from 6 h postdamage and revert to an almost undamaged stage at 24 h post IR (Figures 3b–d). These findings point to NHEJ as the main repair pathway used by human pluripotent stem cells to repair DNA damage caused by IR, corroborating previous findings.[27,28] Overexpression of *DNA LIGASE IV* restores NHEJ activity (Figure 3a) and the ability to respond to IR, albeit not to the same extent as the wild-type control cells (Figures 3b–d).

Under steady state growth (no IR), all LIG4-iPSC lines show a slightly higher level of cells with DSB accumulation, which is likely to be due to reactive oxygen species generation under normoxic culture conditions (Figure 3c). We analysed the impacts of the higher levels of DSBs on proliferation and

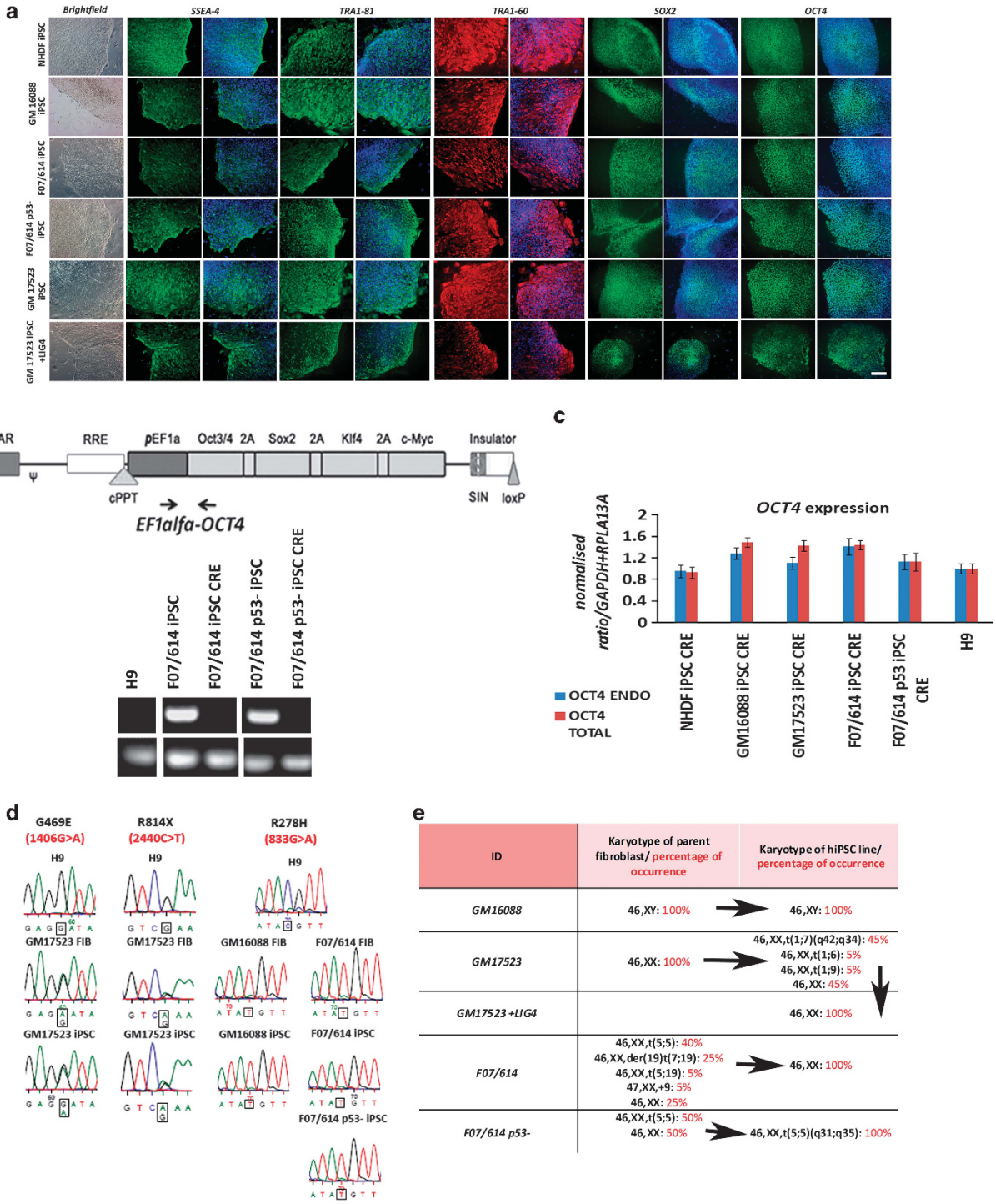

Figure 1 LIG4-iPSC display all the *in vitro* hallmarks of pluripotency and patient-specific genetic mutations. (**a**) Staining of control- and LIG4-iPSC lines with pluripotency cell surface markers (SSEA-4 (green), TRA1-81 (green) and TRA1-60 (red)) and transcription factors (SOX2 (green) and OCT4 (green)). DAPI staining of nuclei is shown in blue (Scale bar = 100 μm); (**b**) Schematic presentation of polycystronic expression construct (OSKM) used for the induction of pluripotency and representative gel electrophoresis used to detect the transgene cassette prior and post Cre excision event; (**c**) Quantitative RT-PCR analysis for the expression of total and endogenous *OCT4* showing removal of exogenous transgene post Cre expression. Data is presented as mean ± S.E.M., $n = 4$. The value for H9 was set to 1 and all other values were calculated with respect to that. CRE = post Cre excision; (**d**) Direct sequencing of cloned PCR products spanning patient-specific mutations in H9 (human ESC control), patient-specific fibroblasts and iPSC lines shows that all LIG4-iPSC lines display the same mutations as fibroblasts isolated from LIG4 patients; (**e**) Summary of karyotype analysis performed in LIG4 fibroblasts and iPSC lines derived from them. Figures highlighted in red indicate the percentage of occurrence amongst 30 metaphases analysed for each sample. Karyotype analysis of fibroblasts was carried out at the same passage used for induction of pluripotency. Human iPSC lines were karyotyped at passage 5 and 15 postderivation. Identical results (shown in this figure) were obtained at both passages

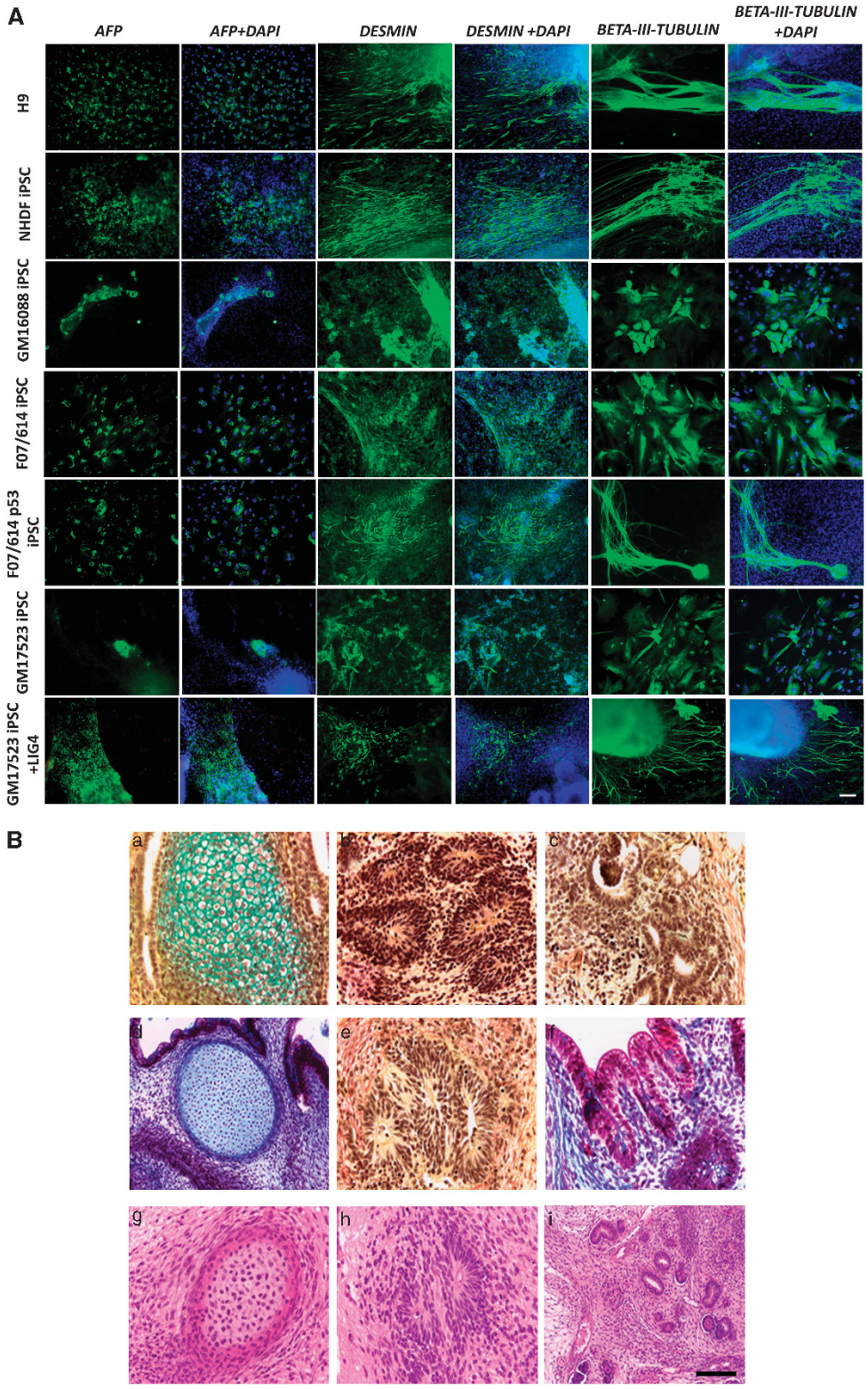

Figure 2 *In vitro* and *in vivo* differentiation capacity of LIG4- and control-iPSC lines. (**A**) *In vitro* differentiation capacity to all three germ layers demonstrated by immunocytochemical staining with an anti-AFP antibody (marker of endoderm), anti-DESMIN antibody (marker of mesoderm) and anti-βIII-Tubulin antibody TUJ1 (marker of ectoderm). DAPI staining of nuclei is shown in blue (Scale bar = 100 μm). (**B**) *In vivo* differentiation capacity of LIG4- and control-iPSC and human ESC lines. Histological analysis of tissue masses formed from grafted colonies of: (**a–c**) human ESC (H9, positive control); (**d–f**) NHDF-iPSC control; (**g–i**) LIG4 overexpressing iPSC line (GM17523 + LIG4). Human ESC, control-iPSC control and *DNA LIGASE IV* overexpressing LIG4 patient-specific iPSC line (GM17523 + LIG4) produced typical large ($\sim$7–10 mm diameter) and diverse teratomas containing structures representative of each germ layer, notably cartilage (**a**, **d**, **g**); neuroepithelium (**b**, **e**, **h**); kidney (**c**, **i**) and profiles of gut wall (**f**). Histological staining: Weigert's (**a–c**, **e**); Masson's Trichrome (**d**, **f**), Hamatoxylin-Eosin (**g**, **h**, **I**). Scale bars: (**a–c**, **e**, **f**, **g**, **h**) 75 μm; (**d**, **I**) 150 μm

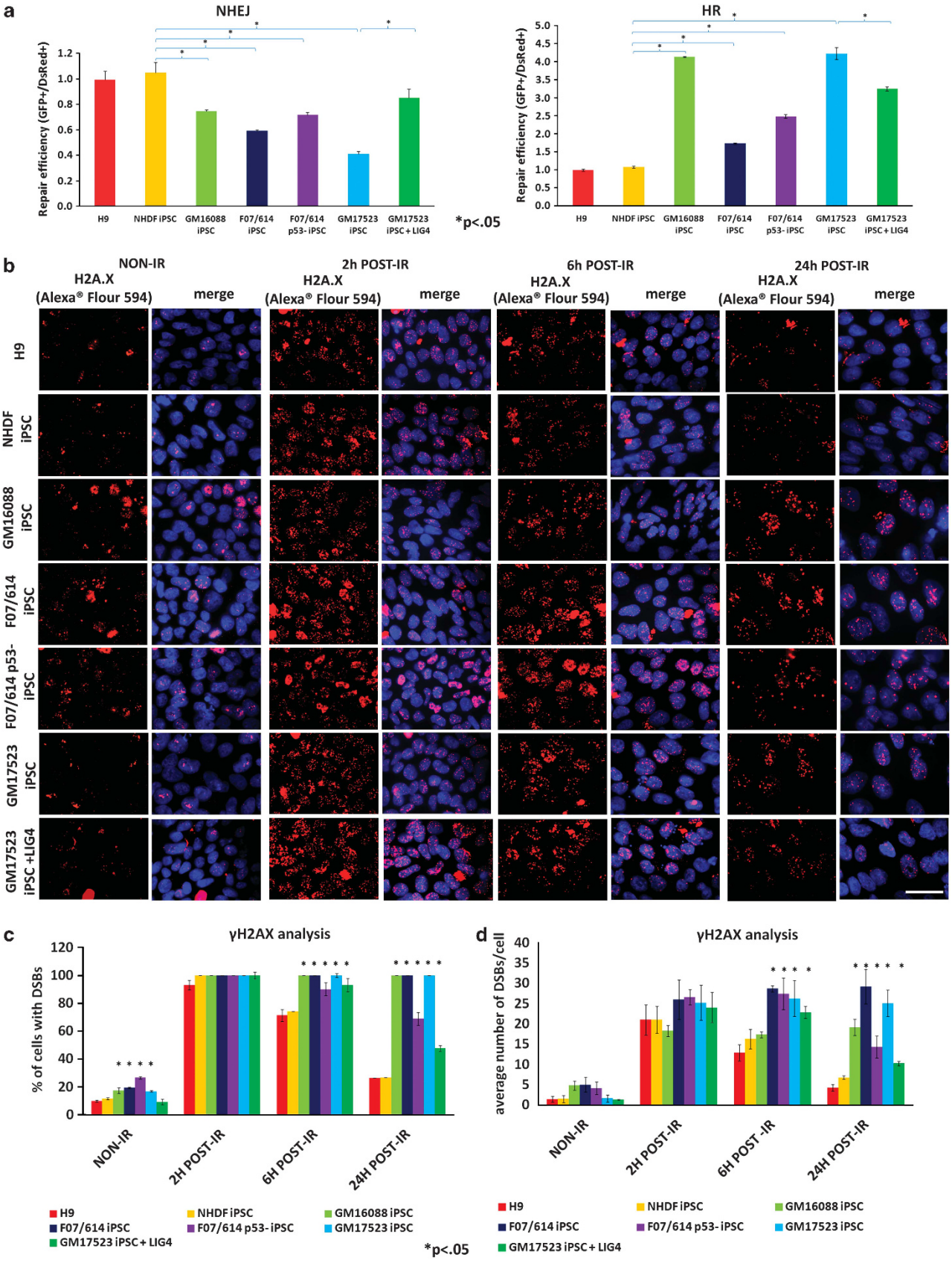
a
NHEJ
Repair efficiency (GFP+/DsRed+)
H9
NHDF iPSC
GM16088 iPSC
F07/614 iPSC
F07/614 p53- iPSC
GM17523 iPSC
GM17523 iPSC + LIG4
*p<.05
HR
b
NON-IR
2h POST-IR
6h POST-IR
24h POST-IR
H2A.X (Alexa® Flour 594)
merge
c
γH2AX analysis
% of cells with DSBs
NON-IR
2H POST-IR
6H POST-IR
24H POST-IR
d
γH2AX analysis
average number of DSBs/cell
6H POST -IR

survival of LIG4-iPSC under normoxic culture conditions and found that despite no changes in their cell cycle profile, apoptosis was enhanced (Supplementary Figures 3A and B). Overexpression of *DNA LIGASE IV* and p53 deficiency rescued the apoptotic phenotype under normoxic culture conditions (Supplementary Figure 3A and data now shown), while IR exacerbated cell death, likely due to accumulation of unrepaired DSBs.

Enhanced apoptosis of LIG4-iPSC was associated with increased expression of apoptotic markers such as BAD, active BAX (data not shown), CASPASE 3 (Supplementary Figure 3C), cleaved CASPASE 3 (Supplementary Figure 3D) and cleaved CASPASE 9 (data not shown), suggesting activation of the intrinsic mitochondrial dependent apoptosis pathway. However, this apoptotic response was reversed in the LIG4-p53- iPSC line despite obvious activation of CASPASE 3 and 9, suggesting the existence of a different pathway in induction of apoptosis. Recently it has been shown that actin-myosin contraction is the major mechanism promoting cell death in human ESC.[34] This process is triggered by the binding of myosin light chain (MLC), which is activated by phosphorylation of Rho-Associated Kinase (ROCK).[35] To investigate whether this pathway was activated in LIG4-iPSC lines we carried ROCK-activity measurement assays (Supplementary Figure 4). This analysis indicated activation of ROCK-dependent signalling in all LIG4-iPSC lines, but not the p53-deficient LIG4-iPSC line (Supplementary Figure 4A), suggesting that activation of p53 pathway is essential for subsequent activation of ROCK-mediated signalling. ROCK activation was accompanied by compaction of the Actin network and increased expression of the phosphorylated form of MLC2 (pMLC2) and both of those were reversed by p53 knockdown (Supplementary Figure 4B). Furthermore, treatment with Blebbistatin (a myosin heavy chain ATPase inhibitor) and Y-27632 (a ROCK inhibitor), reduced apoptosis of all LIG4-iPSC lines (Supplementary Figure 4C), indicating that ROCK activation and contraction of the Actin network is very likely to the p53-dependent pathway, which is activated in LIG4-iPSC lines and leads to the enhancement of apoptotic response.

Impacts of deficient NHEJ-mediated-DSB repair on human iPSC differentiation to haematopoietic lineages. To determine the role of NHEJ-mediated-DSB repair during haematopoietic specification, LIG4- and control-iPSC lines were differentiated in the presence of BMP4, bFGF and VEGF.[36,37] The emergence of haemato-endothelial progenitors (CD34 + CD31 + CD45-), primitive (CD34 + CD45 +) and total blood cells (CD45 +) was analysed by flow cytometry throughout embryoid body (EB) development as described in Real *et al*.[38] Haematopoietic specification from the human ESC line, control- and LIG4-iPSC lines was similar with haemato-endothelial progenitors appearing at day 4 of development and primitive and total blood cells emerging later in the differentiation process (Figure 4a). There was one exception to this: at the later time points of differentiation, LIG4-iPSC lines generated a higher number of haemato-endothelial progenitors, but not primitive and mature blood cells (Figure 4a). This can be explained by the activation of RHO/ROCK signalling in LIG4-iPSC as shown above and recent findings from our group indicating a key role for this pathway in enhancement of haematopoietic differentiation of human ESC.[37] To get further insights into haematopoietic differentiation ability of LIG4- and control-iPSC lines, we carried out colony forming unit (CFUs) assays in semisolid culture. This analysis indicated a significant reduction in the ability of LIG4-iPSC lines to form haematopoietic colonies (Figure 4b). Few colonies were observed for the worst affected LIG4-iPSC lines (GM17523 and F07/614), while the less severely affected GM16088-iPSC line (which shows the highest residual NHEJ activity amongst the three LIG4-iPSC lines) gave similar colony numbers to the control-iPSC and human ESC lines. Secondary replating of the haematopoietic CFUs indicated a similar reduction in the ability of LIG4-iPSC lines to give rise to haematopoietic cells with H9 and control-iPSC showing the highest replating ability (88% for both), followed by the less severe LIG4-iPSC line GM16088 (80%) and the most affected LIG4-iPSC lines, GM17523 and F07/614 (33% and 0%, respectively). These findings suggest that haematopoietic development is likely to vary from one patient to another depending on the levels of residual NHEJ and is corroborated by the clinical data obtained from these three LIG4 patients. Downregulation of p53 did not rescue haematopoietic development in the context of LIG4 deficiency, but the overexpression of *DNA LIGASE IV* reversed the haematopoietic development of GM17523-iPSC line back to levels comparable to control-iPSC and human ESC line, H9 (Figures 4a and b).

The reduced haematopoietic commitment of the two most affected LIG4-iPSC lines (GM17523 and F07/614) could be due to either changes in proliferation of the emerging haematopoietic progenitors or their survival in culture. To address each of these questions we performed flow cytometric analysis on all different haematopoietic cell subpopulations with BrdU to detect cells entering and progressing through S phase, cleaved PARP to detect apoptotic cells and γH2A.X for the detection of DSBs as outlined in Materials and Methods. This analysis revealed that LIG4-iPSC-derived haemato-endothelial progenitors (CD31 + CD34 + CD45 −), primitive (CD34 + CD45 +) and total blood cells (CD45 +)

Figure 3 LIG4-iPSC lines display reduced NHEJ-mediated-DSB repair capacity and increased levels of DSBs under normal and IR conditions. (**a**) Schematic presentation of HR and NHEJ activity, indicating a significant downregulation of NHEJ-DSB repair capacity in LIG4-iPSC lines when compared with control NHDF-iPSC and human ESC lines at 16 h postIR. Data is presented as mean ± S.E.M., $n = 4$. Student's *t*-test was carried out between each LIG4-iPSC and NHDF-iPSC control line to assess significant differences shown by *. (**b**) LIG4-iPSC lines show a greater level of DSB foci (marked by γH2A.X) under normal culture conditions (NON-IR), as well as 2, 6 and 24 h postIR. IR = ionising radiation. This is measured both in terms of cell percentage with DSB foci shown in (**c**) (only cells with more than five foci are counted) and average number of foci per cell shown in (**d**). Data shown in (**c**) and (**d**) is presented as mean ± S.E.M., $n = 4$. Student's *t*-test was carried out between each LIG4-iPSC and NHDF-iPSC control line to assess significant differences shown by *. (**a**–**d**), Overexpression of *DNA LIGASE IV* in GM17523-iPSC restores the NHEJ-DSB repair capacity and results in clearance of DSB caused by IR, albeit not the same extent as the control iPSC and human ESC line

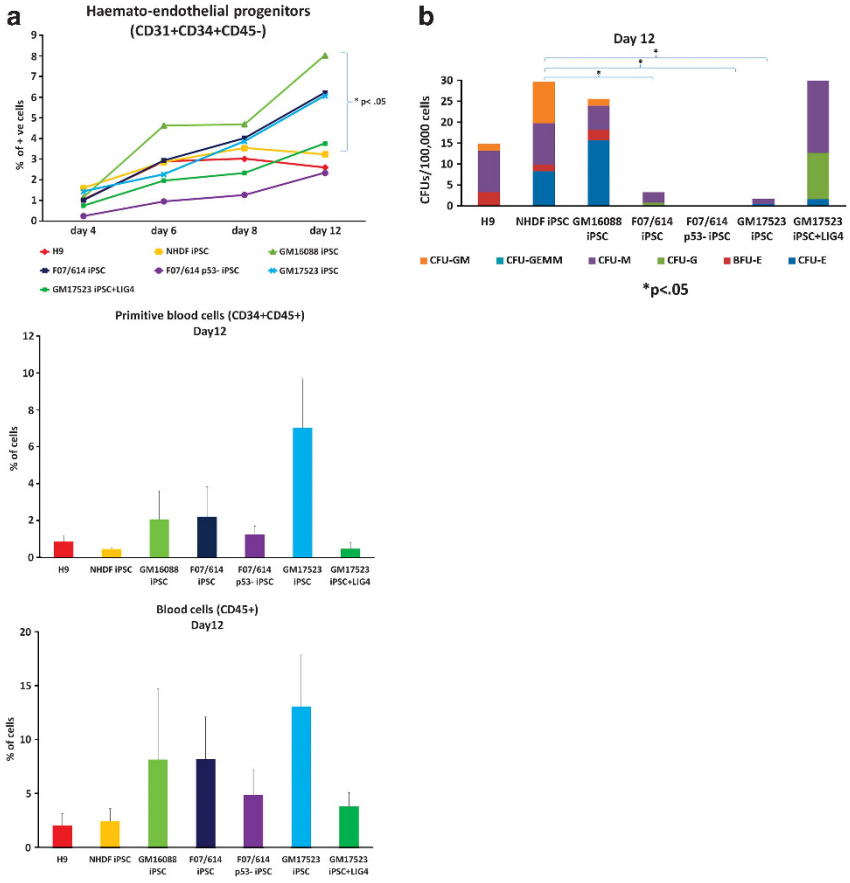

Figure 4 Deficient NHEJ-mediated-DSB repair results in generation of haematopoietic progenitors with reduced clonogenic capacity and differentiation potential. (**a**) LIG4-iPSC undergo haematopoietic differentiation and give rise to haemato-endothelial progenitors (CD31 + CD34 + CD45 −), primitive blood cells (CD34 + CD45 + ; data shown from day 12 of differentiation) and mature blood cells (CD45 + ; data shown from day 12 of differentiation) with similar kinetics to human ESC (H9) and control NHDF-iPSC lines. Data is presented as mean ± S.E.M., $n = 4$. Mann–Whitney *U* test was used to evaluate the differences in the haematopoietic differentiation efficiency between control and LIG4-iPSC lines; (**b**) LIG4-iPSC lines have lower capacity to give rise to haematopoietic colonies in cytokine supplemented semisolid methylcellulose assays. Data is presented at day 12 of differentiation as mean ± S.E.M., $n = 4$. Student's *t*-test was carried out between each LIG4-iPSC and NHDF-iPSC control line to assess significant differences shown by *. Overexpression of *DNA LIGASE IV* restores the ability of GM17523-iPSC to give rise to haematopoietic colonies

retain higher levels of DNA damage (Figure 5a) than equivalent cells from controls. The same analysis on non-haematopoietic cells revealed no significant differences between LIG4- and control-iPSC lines, suggesting that other cell types emerging during the differentiation process may rely on additional mechanisms (for example HR) to repair DNA damage arising under normoxic culture conditions, while emerging haematopoietic progenitors (in particular CD34 + CD45 + which show the highest accumulation of DSBs) rely more heavily on NHEJ-mediated-DSB repair. The increased DNA damage resulted in higher apoptosis of LIG4-iPSC-derived haematopoietic progenitors with CD34 + CD45 + showing the highest apoptotic response, Figure 5b. It is interesting to note that the CD34 + CD45 + subpopulation, which shows the most enhanced apoptotic response and DSB levels, is characterized by enhanced proliferation (Figure 5c), indicating that it is this most proliferating target population that bears the heaviest impact of deficient NHEJ-DSB repair. This higher proliferation, however, could also suggest a feedback loop between higher apoptosis in these cells and demand to replenish the progenitor cell populations. Overexpression of *DNA LIGASE IV* in the GM17523-iPSC line resulted in reduced apoptosis and DNA damage in all haematopoietic progenitors (Figures 5a–c), as well as reduced the cell proliferation of CD34 + CD45 + subpopulation to the levels observed in control NHDF-iPSCs, suggesting that all cellular defects observed in iPSC and emerging haematopoietic progenitors are due specifically to *DNA LIGASE IV* mutations.

Discussion

Gene-knockdown studies in mouse have shown that NHEJ-mediated-DSB repair is important for the survival of haematopoietic and neural progenitors; however, the point at which NHEJ-mediated-DSB repair functions during human embryonic haematopoiesis has not been detailed. Here we report the creation of a human iPSC model of LIG4 deficiency, which accurately replicates the DSB repair phenotype observed in LIG4 patients. Our in depth analysis of haematopoietic differentiation of LIG4-iPSC indicates that impaired NHEJ-mediated-DSB repair impacts survival and proliferation of

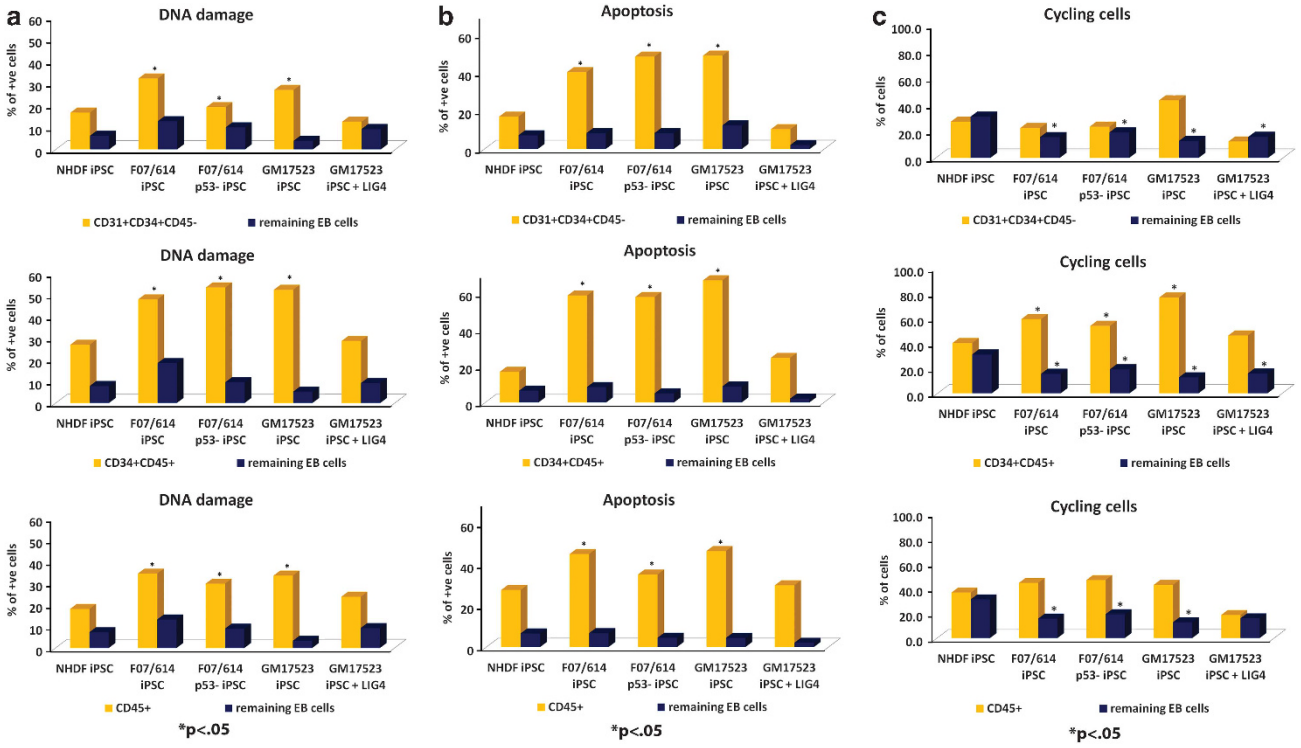

Figure 5 Deficient NHEJ-DSB repair results in increased DNA damage and apoptosis in LIG4-iPSC derived haematopoietic progenitors. (**a**–**c**) Haematopoietic progenitors derived from LIG4-iPSC lines show the highest level of DNA damage (**a**: flow cytometric analysis for phosphorylated H2A.X), highest level of apoptosis (**b**: flow cytometric analysis for measurement of apoptosis with Cleaved PARP) and in some subpopulations enhanced cell proliferation (**c**: flow cytometric analysis for detection of cell proliferation by BrdU) under normal culture conditions. Data is shown as mean of at least four independent experiments. Student's *t*-test was carried out between each LIG4-iPSC and NHDF-iPSC control for each select cell subpopulation to assess significant differences shown by *. All data presented in (**a**–**c**) are from day 12 differentiation. (**a**–**c**) Overexpression of *DNA LIGASE IV* in GM17523-iPSC reduces the accumulation of DSBs, lowers the proliferation and apoptotic haematopoietic progenitors back to levels comparable to progenitors derived from control NHDF-iPSC line

haematopoietic progenitors, rather than haematopoietic differentiation of pluripotent stem cells. Similar findings have been recently reported in the neural progenitor compartment during murine embryonic development where LIG4 deficiency does not affect the neural stem cells residing in the ventricular zone, allowing their transit to the intermediate zone where an apparent sensitivity to persistent DSBs leads to effective apoptosis, reduced progenitor cell numbers and microcephaly.[14] On this basis, we suggest as a working model that the progressive loss of bone marrow cellularity in LIG4 patients is caused by sensitive apoptotic induction from unrepaired DSBs in the haematopoietic progenitor compartment preventing their further differentiation to mature cell types, a key determinant of their ability to maintain themselves against physiological stress and normal metabolism.

Work performed largely in murine ESC has suggested that HR is the preferential mechanism used for DSB repair by ESC.[39] However, recent studies in human ESC and iPSC suggest that this may be different in humans and both HR and NHEJ have a key role in repair of DSBs with specific roles at different stages of cell cycle progression.[27,28] Our results discussed in this manuscript suggest that this is indeed the case for impairment of NHEJ-mediated-DSB repair in human iPSC results in accumulation of DSBs, enhanced apoptosis and increased genomic instability, despite the existence of a functional HR in these cells. On a more practical level, our study raises interesting questions on the ability of iPSC and more broadly embryonic and adult stem cells to preserve their genome integrity during *ex vivo* expansion. Despite enhanced stress defence mechanisms through a combination of elevated removal of reactive oxygen species and reduced ROS production,[26,40] pluripotent stem cells rely heavily on error prone NHEJ to repair IR and culture induced DSBs, which has the potential to lead to genomic instability.[41–45] This has vast implications and warrants further studies to understand and screen DNA repair deficiencies and to define culture conditions that restrict DNA damage and promote *ex vivo* expansion of stem cells without loss of genomic stability.

Recent literature precedence has suggested that activation of certain DNA repair pathways (for example Fanconi Anaemia) is important for somatic cell reprogramming.[46] Although we have not studied in detail whether NHEJ is activated during the reprogramming process; the much lower efficiency of obtaining iPSC from LIG4-NHEJ-deficient fibroblasts together with accumulation of chromosomal abnormalities during the reprogramming of those lines, suggest that activation of NHEJ may also be required in this process. Muller *et al.*[47] have shown that reprogramming induces DNA damage, resulting in upregulation of p53, increased DSBs and senescence. It is possible that NHEJ-deficient fibroblasts may have an increased frequency of DSBs or are less efficient at repairing the DSBs arising during the reprogramming process. Our results with LIG4-iPSC lines suggest that both events are

likely as chromosomal abnormalities were found in some of the LIG4 fibroblasts before the onset of reprogramming but also arose during the reprogramming process and initial culture of some of the LIG4-iPSC. As the field is progressing towards using iPSC-derived cells as autologous source of cells for regenerative medicine, it is worth keeping in mind these genomic instability-associated risks for DNA repair disorders and ensuring that somatic cell to be used for reprogramming are obtained as early as possible and genetically complemented with the functional allele before reprogramming process to ensure maintenance of genomic stability.

Materials and Methods

Cell provision. LIG4-GM17523 and LIG4-GM16088 fibroblasts were purchased from Coriell Cell Repositories. LIG4-F07/614 fibroblasts were obtained from a skin biopsy of a patient in a study approved by the Local Ethics Committee.

iPSC generation. Induction of pluripotency was performed using lentiviral particles encoding all four transcription factors (*OCT4, SOX2, KLF4* and *c-MYC*) under a single polycystronic cassette (Allele Biotech, San Diego, CA, USA). Briefly, 2×10^4 fibroblasts were seeded onto one well of a 12-well plate and cultured as indicated above. The cells were then infected with lentiviral particles (MOI = 0.5) with addition of 6 μg/ml polybrene. Six days after transduction, fibroblasts were disaggregated to single cells by trypsinisation (0.05% Trypsin, Invitrogen, Carlsbad, CA, USA) and plated onto feeder layers of mitotically inactivated mouse embryonic fibroblasts in human ESC culture medium at a density of 8000 cells per one well of a six-well plate. The feeder plates with lentiviral particle-treated cells were maintained at 37 °C, 5% CO_2 in human ESC/iPSC medium for 21 days or until colonies of cells with morphology similar to human ESC appeared. A second step of transgene removal was performed by transfecting human iPSC with Puro.Cre expression construct (Addgene, Plasmid no. 17408) and selecting stable clones with puromycin selection (0.6 μg/ml). Overexpression of *DNA LIGASE IV* was performed by transfecting LIG4-iPSC with the full length *DNA LIGASE IV* cDNA clone (OmicsLink Expression clone, cat. no: EX-T8254-Lv41) and selecting stable clones by geneticin selection (200 μg/ml).

Cell culture. Dermal fibroblasts were cultured in tissue culture coated flasks (Iwaki T25) in Iscove's Modified Dulbecco's Medium, 10% fetal calf serum (PAA), 2 mM L-glutamine (PAA), 1% nonessential amino acids (PAA), 100 units/ml penicillin (PAA) at 37 °C and 5% CO_2. Human ESC (H9) and iPSC lines were cultured as discrete colonies on feeder layers of mitotically inactivated mouse embryonic fibroblasts as previously described.[48] Monolayer and EB differentiation were induced as previously described.[48]

Haematopoietic differentiation. In brief, human ESC and iPSC clumps were allowed to form EBs in StemPro-34 Serum-free media (Invitrogen) supplemented with BMP4 (100 ng/ml), monothioglycerol (4×10^{-4} M) and ascorbic acid (50 μg/ml) for 24 h. A medium change was performed and EBs were resuspended in StemPro-34 Serum-free media supplemented with 100 ng/ml BMP4 (Peprotech, Rocky Hill, NJ, USA), 4×10^{-4} M monothioglycerol (Sigma-Aldrich, St. Louis, CO, USA), 50 μg/ml ascorbic acid (Sigma-Aldrich) and 10 ng/ml bFGF (Invitrogen) for 72 h as previously described. In the final step of differentiation, EBs were resuspended in StemPro-34 Serum-free media (Invitrogen) supplemented with 100 ng/ml BMP4 (Peprotech), 4×10^{-4} M monothioglycerol (Sigma-Aldrich), 50 μg/ml ascorbic acid (Sigma-Aldrich), 5 ng/ml bFGF (Invitrogen) and 10 ng/ml VEGF (Peprotech) with the media changed every 2 days.

Haematopoietic colony assays. All haematopoietic progenitor assays were performed according to manufacturer's instructions using MethoCult GF H4434 (Stem Cell Technologies, Vancouver, BC, Canada). After 12–14 days incubation at 37 °C, 5% CO_2 in humidified atmosphere, the plates were scored for CFU-G, CFU-M, CFU-GM, CFU-E, BFU-E and CFU-GEMM colonies under light microscope.

Flow cytometric analysis of haematopoietic specification. The antibodies used in this study were: anti-CD34-PE-Cy7 (cat. no: 56710; BD Pharmingen, Franklin Lakes, NJ, USA), anti-CD31-APC-eFluor780 (cat. no: 47-0319; E-Bioscience, San Diego, CA, USA) and CD45-FITC (cat. no: 555482; BD Pharmingen). Appropriate corresponding IgG/M isotype controls were used in all experiments. The cells were washed with PBS to remove excess antibodies and resuspended in 500 μl of PBS with 5% fetal calf serum. Ten microliters of 4′, 6-diamidino-2-phenylindole (DAPI; Sigma-Aldrich) were added to the sample and incubated in the dark at room temperature for 30 min. The cells were washed with PBS to remove excess stain and resuspended in 500 μl of PBS with 5% FBS and ready to be put through a flow cytometer for analysis (BD FACS LSRII) using DIVA software (BD, Franklin Lakes, NJ, USA).

Immunofluorescence. Human iPSC and ESC were fixed in 4% (w/v) paraformaldehyde for 20 min. An additional permeabilisation step (0.2% (v/v) Triton X-100 in PBS) was performed before staining with antibodies for internal cell markers. Blocking step was performed by incubation in 1% (w/v) BSA or alternatively in 10% (v/v) goat serum. Cells were incubated with primary antibodies for 1 h and secondary antibodies for 30–60 min. Primary antibodies used in this study are anti-OCT4, (cat. no. IC1759F; 1 : 100; R&D Systems, Minneapolis, MN, USA), anti-DESMIN (ab 15200-1; 1 : 100, Abcam, Cambridge, UK), anti-alpha-fetoprotein (MAB 1369; 1 : 100; R&D Systems), anti-SOX2 (cat no. 560301; 1 : 100: BD Biosciences), anti-SSEA-4 (cat. no. 560073; 1 : 100; BD Bioscience), anti-TRA-181 (cat. no. MAB43181; 1 : 100; Millipore, Darmstadt, Germany), anti-TRA-1-60 (MAB4381: 1 : 100; Millipore), anti-β-III-Tubulin (TUJ1) (cat. no. MMS-435P; 1 : 100; Covance, Princeton, NJ, USA) and various anti-mouse or anti-rat IgG/IgM-FITC or TRITC conjugated (1 : 200; all from Sigma-Aldrich). The nuclei were counterstained with DAPI (Invitrogen). The bright field and fluorescent images were obtained using a Zeiss microscope and the AxioVision software (Carl Zeiss, Oberkochen, Germany).

Western immunoblotting. Protein extraction and western blotting were performed as published previously.[49] Primary antibodies included Caspase 3 (H-277, Santa Cruz Biotechnology Inc., Santa Cruz, CA, USA; 1 : 100 dilution), Bad (H-168, Santa Cruz Biotechnology Inc., 1 : 100 dilution) and DNA LIGASE IV (Santa Cruz Biotechnology, Inc., H-300, dilution 1 : 200). The antibody to GAPDH (Abcam, ab9485: 1 : 100 dilution) was used after membrane stripping to confirm uniform protein loading. Antibody/antigen complexes were detected using ECL (Amersham Biosciences, Buckinghamshire, UK) and images were acquired using a luminescent image analyser FUJIFILM and LAS-3000 software (FUJI, Tokyo, Japan).

Quantitative RT-PCR. Total RNA was extracted using TRIzol reagent (Invitrogen) according to manufacturer's instructions. Following DNase*I* treatment using RQ1 DNaseI (Promega, Fitchburg, WI, USA), cDNA was synthesised using SuperScript Reverse Transcriptase (Invitrogen). Quantitative RT-PCR analysis was carried out using SYBR Green PCR master mix (Sigma-Aldrich) and the following oligonucleotides: *OCT4* TOTAL forward: 5′-GAGGAGTCCCAGGACATC AA-3′; *OCT4* TOTAL reverse: 5′-CATCGGCCTGTGTATATCCC-3′; *OCT4* endogenous forward: 5′-AAGCCCTCATTTCACCAGGCC-3′: *OCT4* endogenous reverse: 5′-CTTGGAAGCTTAGCCAGGTC-3′; p*EF1*α forward: 5′-TCAAGCCTCA GACAGTGGTTC-3′, *OCT4* reverse: 5′-CATCGGCCTGTGTATATCCC-3′, *p53* forward 5′-AAGACCTGCCCTGTG and *p53* reverse 5′-TGACGCACACCTATTG CAAG. All reactions were carried out in four replicates and samples were analysed using an AB7900HT real-time analyzer. Data were analysed using qBase v1.3.5 and the comparative threshold cycle (C_t) method. In all samples the results were normalised to two housekeeping genes (hkg) *GAPDH* and *RPL13A* as described previously.[50]

Cell cycle analysis. Human ESC and iPSC were collected using Accutase (Chemicon, Temecula, CA, USA). Cell cycle analysis was performed using the CycleTest Plus DNA reagent kit (Becton Dickinson, Franklin Lakes, NJ, USA) with FACS Calibur (BD Biosciences). The data were analyzed using FlowJo software (Tree Star, Ashland, OR, USA) to generate percentages of cells in G1, S and G2/M phases.

DSB quantification by γH2A.X staining. Cells grown in coverslips were fixed in 1 ml of 2% paraformaldehyde in PBS for 10 min at room temperature. Paraformaldehyde was removed and cells were washed twice with PBS. Cell permeabilisation was carried out by incubation for 45 min at room temperature with 1 ml PBG-Triton. Primary antibody against phosphorylated γ-H2A.X mouse monoclonal anti-phospho histone H2A.X (Ser 139, Upstate) was added and cells were incubated for 1 h at room temperature with gentle agitation. Cells

were washed twice with PBG and further incubated for 45 min to 1 h with fluorescein-conjugated secondary antibody (Alexa Fluor 594), then washed three times with PBS for 5 min. Cells were stained for 10 min with 400 μl of DAPI. After DAPI staining, the washing step was repeated before mounting cells on slides using an anti-fade mounting medium (Vecta Shield). Slides were examined using a Zeiss Axioplan microscope. Quantification was performed using Image J by counting γH2A.X positive foci in 150–200 nuclei per experiment.

Flow cytometric analysis for assessing apoptosis, DNA damage and cell proliferation. This was performed using a flow cytometric kit (cat. no. 562253; BD Biosciences) and following manufacturer's instructions. In brief, human ESC and iPSC were labelled with BrdU, stained with antibodies to cell surface markers (CD31,CD34,C45), then fixed, permeabilized and treated with DNAse*I*. Following this treatment, cells were simultaneously stained with PerCP-Cy5.5 labelled BrdU, PE labelled anti-cleaved PARP and Alexa Fluor 647 labelled anti–γH2AX. Cells were resuspended in staining buffer and analysed by flow cytometry. At least 10 000 events were recorded for each sample.

Validation of known LIG4 patient mutations in iPSCs. To validate the mutations found in the LIG4- patient's peripheral blood DNA, sequences were amplified using the following primers: LIG4_MUT 1406 forward: 5′-GCCAGACA AAAGAGGTGAAGGGTGG-3′, LIG4_ MUT 1406 reverse: 5′-AGGGGGCTTC TCTGCTACTGCA-3′, LIG4_MUT 2440 forward: 5′-ACGAGCAGACTCCTGAAG AAATGGCT-3′, LIG4_MUT 2440 reverse: 5′-CCATGAAACCGAAGCTCCAAG GC-3′, LIG4_MUT 833 forward: 5′-GCTAGCTGCTATTGCAGATATTGAGC-3′ and LIG4_MUT 833 reverse: 5′-AGAACCTTCAGTAGGAGAAGCACCAA-3′. LIG4-PCR products were subcloned into TOPO XL (Invitrogen AG, Basel, Switzerland) and sequenced using an ABI Prism Genetic Analyzer (Applied Biosystems Deutschland GmbH, Darmstadt, Germany). At least five clones were sequenced in both directions to confirm DNA sequence.

Karyotype analysis. Karyotypes were determined by standard G-banding procedure as described previously.[48] At least 30 metaphases were analysed for each sample.

Teratoma formation. A total of 5×10^5 iPSC were injected subcutaneously into the right flank of an adult SCID mice and maintained for 8–12 weeks.[48] Similarly, for a positive control, 5×10^5 human ESC (H9 cell line) were injected subcutaneously in adult SCID male mice. All cells were cotransplanted with 50 μl Matrigel (BD Biosciences) to enhance teratoma formation. Four to six animals were injected in each group. After 8–12 weeks, mice were killed, tissues were dissected, fixed in Bouins overnight, processed and sectioned according to standard procedures and counterstained with either haematoxylin and eosin or Massons Trichrome stain. Sections (5–8 μm) were examined using bright field light microscopy and photographed as appropriate.

RNA interference. Downregulation of *p53* in LIG4 fibroblasts was carried out using ready-made lentiviral particles (MOI = 0.5) encoding two specific p53 shRNAs embedded within the pLKO.1-puro vector (Clone ID: TRCN0000003756 AND TRCN0000010814, Sigma-Aldrich) and selecting stable single clones by application of geneticin (200 μg/ml).

Measurement of ROCK activity. This was performed using a 96-well ROCK activity Assay Kit (Cell Biolab's, San Diego, CA, USA; cat. no. TA-416), which relies on detection of specific phosphorylation of MYPT1 at Th696 by ROCK. Cell Lysates were incubated in wells coated with recombinant MYPT1 and detection of phosphorylated MYPT1 was carried out using an anti-phospho-MYPT1 (Th696) antibody. Absorbance from each well was recorded using a spectrophotometer at 450 nm.

Analysis of DSB repair. This analysis was carried out using the fluorescent reporter constructs that enable sensitive and quantitative measurement of NHEJ and HR activity.[31] These constructs (kind gift of Dr Vera Gorbunova) are based on an engineered GFP gene containing rare-cutting *I*-SceI endonuclease for induction of DSBs and that is inactivated either by an additional exon or by mutations. Repair of the *I*-SceI induce breaks by NHEJ or HR restores the functional GFP gene. Both constructs were transfected into human ESC and iPSC using nucleofection as described in our previous publication. A control transfection with pDsRed2-N1 Vector (cat. no. 632406; Clontech, Mountain View, CA, USA) was performed to estimate transfection efficiency of each cell type. The number of GFP and RFP positive cells was analysed by flow cytometry and plotted as a ratio.

Conflict of Interest

The authors declare no conflict of interest.

Acknowledgements. The authors would like to thank Mr Ian Dimmick and Dr Owen Hughes for their help with the flow cytometric analysis, Dr. Josef Jaros for help with the work on cytoskeleton and ROCK signalling, Complement Genomics plc. for carrying out the DNA fingerprinting analysis, Addgene for provision of the Cre construct and Coriell Cell Repositories for providing some of the LIG4 patient fibroblasts. This study was supported by Leukamia and Lymphoma Research Grant 09005 and funds for research in the field of Regenerative Medicine through the collaboration agreement from the Conselleria de Sanidad (Generalitat Valenciana) and the Instituto de Salud Carlos III (Ministry of Science and Innovation), Spain.

Author contributions:

Katarzyna Tilgner: performed the majority of experiments, data collection and analysis, contribution to manuscript writing, final approval of manuscript. Irina Neganova, Inmaculada Moreno-Gimeno, Deborah Burks, Sun Yung, Jerome Evans, Gabriele Saretzki, Chatchawan Singhapol: performed some of the experiments, final approval of manuscript. Jumana Yousuf AL-Aama: provided important reagents for this work, performed some of the experiments, final approval of manuscript. Vera Gorbunova: provided important reagents for this work, final approval of manuscript. Andrew Gennery: conception and design of the study, provided important reagents for this work, final approval of manuscript. Stefan Przyborski: performed some of the experiments, collection and analysis of the data, contributed to manuscript writing and final approval of manuscript. Miodrag Stojkovic, Lyle Armstrong: conception and design, manuscript writing, fund raising and final approval of manuscript. Penny Jeggo: provided reagents for this work, design, data analysis, manuscript writing, fund raising and final approval of manuscript. Majlinda Lako: conception and design, performed experiments, data analysis, manuscript writing, fund raising and final approval of manuscript.

1. Hartlerode AJ, Scully R. Mechanisms of double-strand break repair in somatic mammalian cells. *Biochem J* 2009; **423**: 157–168.
2. Jeggo PA. DNA breakage and repair. *Adv Genet* 1998; **38**: 185–218.
3. Holthausen JT, Wyman C, Kanaar R. Regulation of DNA strand exchange in homologous recombination. *DNA Repair (Amst)* 2010; **9**: 1264–1272.
4. Lieber MR, Ma Y, Pannicke U, Schwarz K. Mechanism and regulation of human non-homologous DNA end-joining. *Nat Rev Mol Cell Biol* 2003; **4**: 712–720.
5. Grawunder U, Grawunder U, Wilm M, Wu M, Kulesza P, Wilson TE *et al.* Activity of DNA ligase IV stimulated by complex formation with XRCC4 protein in mammalian cells. *Nature* 1997; **388**: 492–495.
6. Ahnesorg P, Smith P, Jackson SP. XLF interacts with the XRCC4-DNA ligase IV complex to promote DNA nonhomologous end-joining. *Cell* 2006; **124**: 301–313.
7. Nussenzweig A, Nussenzweig MC. A backup DNA repair pathway moves to the forefront. *Cell* 2007; **131**: 223–225.
8. Jackson SP, Bartek J. The DNA-damage response in human biology and disease. *Nature* 2009; **461**: 1071–1078.
9. O'Driscoll M, Gennery AR, Seidel J, Concannon P, Jeggo PA. An overview of three new disorders associated with genetic instability: LIG4 syndrome, RS-SCID and ATR-Seckel syndrome. *DNA Repair (Amst)* 2004; **3**: 1227–1235.
10. Frank KM, Sekiguchi JM, Seidl KJ, Swat W, Rathbun GA, Cheng HL *et al.* Late embryonic lethality and impaired V(D)J recombination in mice lacking DNA ligase IV. *Nature* 1998; **396**: 173–177.
11. Frank KM, Sharpless NE, Gao Y, Sekiguchi JM, Ferguson DO, Zhu C *et al.* DNA ligase IV deficiency in mice leads to defective neurogenesis and embryonic lethality via the p53 pathway. *Mol Cell* 2000; **5**: 993–1002.
12. Gao Y, Sun Y, Frank KM, Dikkes P, Fujiwara Y, Seidl KJ *et al.* A critical role for DNA end-joining proteins in both lymphogenesis and neurogenesis. *Cell* 1998; **95**: 891–902.
13. Nijnik A, Woodbine L, Marchetti C, Dawson S, Lambe T, Liu C *et al.* DNA repair is limiting for haematopoietic stem cells during ageing. *Nature* 2007; **447**: 686–690.
14. Gatz SA, Ju L, Gruber R, Hoffmann E, Carr AM, Wang ZQ *et al.* Requirement for DNA ligase IV during embryonic neural development. *J Neurosci* 2011; **31**: 10088–10100.
15. O'Driscoll M, Cerosaletti KM, Girard PM, Dai Y, Stumm M, Kysela B *et al.* DNA ligase IV mutations identified in patients exhibiting developmental delay and immunodeficiency. *Mol Cell* 2001; **8**: 1175–1185.
16. Riballo E, Critchlow SE, Teo SH, Doherty AJ, Priestley A, Broughton B *et al.* Identification of a defect in DNA ligase IV in a radiosensitive leukaemia patient. *Curr Biol* 1999; **9**: 699–702.

17. Ben-Omran TI, Cerosaletti K, Concannon P, Weitzman S, Nezarati MM. A patient with mutations in DNA Ligase IV: clinical features and overlap with Nijmegen breakage syndrome. *Am J Med Genet A* 2005; **137A**: 283–287.
18. Chistiakov DA. Ligase IV syndrome chapter 16: 175-183: Diseases of DNA repair, edited by S. I. Ahmad.
19. Rossi DJ, Bryder D, Seita J, Nussenzweig A, Hoeijmakers J, Weissman IL. Deficiencies in DNA damage repair limit the function of haematopoietic stem cells with age. *Nature* 2007; **447**: 725–729.
20. Zhang S, Yajima H, Huynh H, Zheng J, Callen E, Chen HT *et al.* Congenital bone marrow failure in DNA-PKcs mutant mice associated with deficiencies in DNA repair. *J Cell Biol* 2011; **193**: 295–305.
21. Lucas D, Escudero B, Ligos JM, Segovia JC, Estrada JC, Terrados G *et al.* Altered hematopoiesis in mice lacking DNA polymerase mu is due to inefficient double-strand break repair. *PLoS Genet* 2009; **5**: e1000389.
22. Nijnik A, Dawson S, Crockford TL, Woodbine L, Visetnoi S, Bennett S *et al.* Impaired lymphocyte development and antibody class switching and increased malignancy in a murine model of DNA ligase IV syndrome. *J Clin Invest* 2009; **119**: 1696–1705.
23. Rucci F, Notarangelo LD, Fazeli A, Patrizi L, Hickernell T, Paganini T *et al.* Homozygous DNA ligase IV R278H mutation in mice leads to leaky SCID and represents a model for human LIG4 syndrome. *Proc Natl Acad Sci USA* 2010; **107**: 3024–3029.
24. Mohrin M, Bourke E, Alexander D, Warr MR, Barry-Holson K, Le Beau MM *et al.* Hematopoietic stem cell quiescence promotes error-prone DNA repair and mutagenesis. *Cell Stem Cell* 2010; **7**: 174–185.
25. Saretzki G, Armstrong L, Leake A, Lako M, von Zglinicki T. Stress defense in murine embryonic stem cells is superior to that of various differentiated murine cells. *Stem Cells* 2004; **22**: 962–971.
26. Saretzki G, Walter T, Atkinson S, Passos JF, Bareth B, Keith WN *et al.* Downregulation of multiple stress defence mechanisms during differentiation of human embryonic stem cells. *Stem Cells* 2008; **26**: 455–464.
27. Bogomazova AN, Lagarkova MA, Tskhovrebova LV, Shutova MV, Kiselev SL. Error-prone nonhomologous end joining repair operates in human pluripotent stem cells during late G2. *Aging* 2011; **3**: 584–596.
28. Fan J, Robert C, Jang YY, Liu H, Sharkis S, Baylin SB *et al.* Human induced pluripotent cells resemble embryonic stem cells demonstrating enhanced levels of DNA repair and efficacy of nonhomologous end-joining. *Mutat Res* 2011; **713**: 8–17.
29. Roddam PL, Rollinson S, O'Driscoll M, Jeggo PA, Jack A, Morgan GJ. Genetic variants of NHEJ DNA ligase IV can affect the risk of developing multiple myeloma, a tumour characterised by aberrant class switch recombination. *J Med Genet* 2002; **39**: 900–905.
30. Marión RM, Strati K, Li H, Murga M, Blanco R, Ortega S *et al.* A p53-mediated DNA damage response limits reprogramming to ensure iPS cell genomic integrity. *Nature* 2009; **460**: 1149–1153.
31. Seluanov A, Mao Z, Gorbunova V. Analysis of DNA double-strand break (DSB) repair in mammalian cells. *J Vis Exp* 2002; **43,** pii 2002.
32. Delacôte F, Han M, Stamato TD, Jasin M, Lopez BS. An xrcc4 defect or Wortmannin stimulates homologous recombination specifically induced by double-strand breaks in mammalian cells. *Nuc Acids Res* 2002; **30**: 3454–3463.
33. Pierce AJ, Hu P, Han M, Ellis N, Jasin M. Ku DNA end-binding protein modulates homologous repair of double-strand breaks in mammalian cells. *Genes Dev* 2001; **15**: 3237–3242.
34. Ohgushi M, Matsumura M, Eiraku M, Murakami K, Aramaki T, Nishiyama A *et al.* Molecular pathway and cell state responsible for dissociation-induced apoptosis in human pluripotent stem cells. *Cell Stem Cell* 2010; **7**: 225–239.
35. Chen G, Hou Z, Gulbranson DR, Thomson JA. Actin-myosin contractility is responsible for the reduced viability of dissociated human embryonic stem cells. *Cell Stem Cell* 2010; **7**: 240–248.
36. Kennedy M, D'Souza SL, Lynch-Kattman M, Schwantz S, Keller G. Development of the hemangioblast defines the onset of hematopoiesis in human ES cell differentiation cultures. *Blood* 2007; **109**: 2679–2687.
37. Yung S, Ledran M, Moreno-Gimeno I, Conesa A, Montaner D, Dopazo J *et al.* Large-scale transcriptional profiling and functional assays reveal important roles for Rho-GTPase signalling and SCL during haematopoietic differentiation of human embryonic stem cells. *Hum Mol Genet* 2011; **20**: 4932–4946.
38. Real PJ, Ligero G, Ayllon V, Ramos-Mejia V, Bueno C, Gutierrez-Aranda I *et al.* SCL/TAL1 regulates hematopoietic specification from human embryonic stem cells. *Mol Ther* 2012; **20**: 1443–1453.
39. Bañuelos CA, Banáth JP, MacPhail SH, Zhao J, Eaves CA, O'Connor MD *et al.* Mouse but not human embryonic stem cells are deficient in rejoining of ionizing radiation-induced DNA double-strand breaks. *DNA Repair (Amst)* 2008; **7**: 1471–1483.
40. Armstrong L, Tilgner K, Saretzki G, Atkinson SP, Stojkovic M, Moreno R *et al.* Human induced pluripotent stem cell lines show stress defense mechanisms and mitochondrial regulation similar to those of human embryonic stem cells. *Stem Cells* 2010; **28**: 661–673.
41. Mayshar Y, Ben-David U, Lavon N, Biancotti JC, Yakir B, Clark AT *et al.* Identification and classification of chromosomal aberrations in human induced pluripotent stem cells. *Cell Stem Cell* 2010; **7**: 521–531.
42. Elliott AM, Elliott KA, Kammesheidt A. High resolution array-CGH characterization of human stem cells using a stem cell focused microarray. *Mol Biotech* 2010; **46**: 234–242.
43. Laurent LC, Ulitsky I, Slavin I, Tran H, Schork A, Morey R *et al.* Dynamic changes in the copy number of pluripotency and cell proliferation genes in human ESCs and iPSCs during reprogramming and time in culture. *Cell Stem Cell* 2011; **8**: 106–118.
44. International Stem Cell InitiativeAmps K, Andrews PW, Anyfantis G, Armstrong L, Avery S, Baharvand H *et al.* Screening ethnically diverse human embryonic stem cells identifies a chromosome 20 minimal amplicon conferring growth advantage. *Nat Biotech* 2011; **29**: 1132–1144.
45. Martins-Taylor K, Nisler BS, Taapken SM, Compton T, Crandall L, Montgomery KD *et al.* Recurrent copy number variations in human induced pluripotent stem cells. *Nat Biotech* 2011; **29**: 488–491.
46. Yung SK, Tilgner K, Ledran MH, Habibollah S, Neganova I, Singhapol C *et al.* Human pluripotent stem cell models of Fanconi Anaemia deficiency reveal an important role for Fanconi Anaemia proteins in cellular reprogramming and survival of haematopoietic progenitors. *Stem Cells* 2013; **31**: 1022–1029.
47. Müller LU, Milsom MD, Harris CE, Vyas R, Brumme KM, Parmar K *et al.* Overcoming reprogramming resistance of Fanconi anemia cells. *Blood* 2012; **119**: 5449–5457.
48. Stojkovic M, Lako M, Stojkovic P, Stewart R, Przyborski S, Armstrong L *et al.* Derivation of human embryonic stem cells from day-8 blastocysts recovered after three-step in vitro culture. *Stem Cells* 2004; **22**: 790–797.
49. Neganova I, Zhang X, Atkinson S, Lako M. Expression and functional analysis of G1 to S regulatory components reveals an important role for CDK2 in cell cycle regulation in human embryonic stem cells. *Oncogene* 2008; **28**: 20–30.
50. Mellough CB, Sernagor E, Moreno-Gimeno I, Steel DH, Lako M. Efficient stage-specific differentiation of human pluripotent stem cells toward retinal photoreceptor cells. *Stem Cells* 2012; **30**: 673–686.

Supplementary Information accompanies this paper on Cell Death and Differentiation website (http://www.nature.com/cdd)